

AD-A045 073

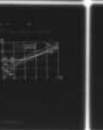
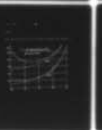
FOREIGN TECHNOLOGY DIV WRIGHT-PATTERSON AFB OHIO
INVESTIGATION OF VELOCITY FIELD BEHIND LOW-FLYING WING WITH FUS--ETC(U)
MAY 77 M K BOCHIN, L G TSVETKOV
FTN-IN(RS)I-0531-77

F/G 20/4

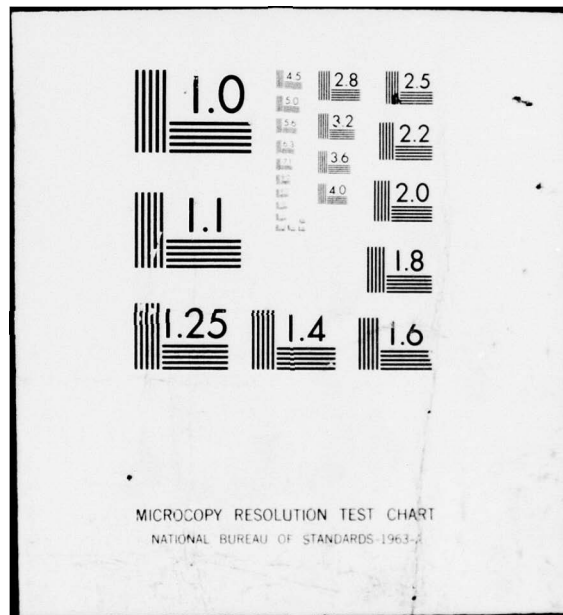
UNCLASSIFIED

NL

1 OF 1
AD
A045 073



END
DATE
FILMED
11-77
DDC



AD-A045073

1

FOREIGN TECHNOLOGY DIVISION



INVESTIGATION OF VELOCITY FIELD BEHIND LOW-FLYING
WING WITH FUSELAGE

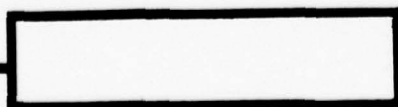
by

M. K. Bochin, L. G. Tsvetkov



DDDC
RECEIVED
OCT 11 1977
D

Approved for public release;
distribution unlimited.



ADDITIONAL INFO	
RTIC	Write Section <input checked="" type="checkbox"/>
DDC	Self Section <input type="checkbox"/>
UNCLASSIFIED	<input type="checkbox"/>
JUSTIFICATION	
BY	
DISTRIBUTION/AVAILABILITY CODES	
Dist.	AVAIL. and/or SPECIAL
A	EC

FTD-ID(RS)I-0531-77

EDITED TRANSLATION

FTD-ID(RS)I-0531-77

11 May 1977

AD-77-C-000511

INVESTIGATION OF VELOCITY FIELD BEHIND LOW-FLYING
WING WITH FUSELAGE

By: M. K. Bochin, L. G. Tsvetkov

English pages: 16

Source: Trudy Leningradskogo Korablestroitel'nogo
Instituta, Leningrad, Vol 69, 1970, PP.11-
17

Country of origin: USSR

Translated by: Marilyn Olacchia

Requester: FTD/PDRS

Approved for public release; distribution unlimited.

THIS TRANSLATION IS A RENDITION OF THE ORIGINAL FOREIGN TEXT WITHOUT ANY ANALYTICAL OR EDITORIAL COMMENT. STATEMENTS OR THEORIES ADVOCATED OR IMPLIED ARE THOSE OF THE SOURCE AND DO NOT NECESSARILY REFLECT THE POSITION OR OPINION OF THE FOREIGN TECHNOLOGY DIVISION.

PREPARED BY:

TRANSLATION DIVISION
FOREIGN TECHNOLOGY DIVISION
WP-AFB, OHIO.

FTD-ID(RS)I-0531-77

Date 11 May 19 77

U. S. BOARD ON GEOGRAPHIC NAMES TRANSLITERATION SYSTEM

Block	Italic	Transliteration	Block	Italic	Transliteration
А а	<i>А а</i>	A, a	Р р	<i>Р р</i>	R, r
Б б	<i>Б б</i>	B, b	С с	<i>С с</i>	S, s
В в	<i>В в</i>	V, v	Т т	<i>Т т</i>	T, t
Г г	<i>Г г</i>	G, g	У у	<i>У у</i>	U, u
Д д	<i>Д д</i>	D, d	Ф ф	<i>Ф ф</i>	F, f
Е е	<i>Е е</i>	Ye, ye; E, e*	Х х	<i>Х х</i>	Kh, kh
Ж ж	<i>Ж ж</i>	Zh, zh	Ц ц	<i>Ц ц</i>	Ts, ts
З з	<i>З з</i>	Z, z	Ч ч	<i>Ч ч</i>	Ch, ch
И и	<i>И и</i>	I, i	Ш ш	<i>Ш ш</i>	Sh, sh
Й й	<i>Й й</i>	Y, y	Щ щ	<i>Щ щ</i>	Shch, shch
К к	<i>К к</i>	K, k	Ъ ъ	<i>Ъ ъ</i>	"
Л л	<i>Л л</i>	L, l	Ы ы	<i>Ы ы</i>	Y, y
М м	<i>М м</i>	M, m	Ь ь	<i>Ь ь</i>	'
Н н	<i>Н н</i>	N, n	Э э	<i>Э э</i>	E, e
О о	<i>О о</i>	O, o	Ю ю	<i>Ю ю</i>	Yu, yu
П п	<i>П п</i>	P, p	Я я	<i>Я я</i>	Ya, ya

*ye initially, after vowels, and after ъ, ь; e elsewhere.
 When written as ё in Russian, transliterate as yě or ë.
 The use of diacritical marks is preferred, but such marks may be omitted when expediency dictates.

GREEK ALPHABET

Alpha	A	α	α	Nu	Ν	ν
Beta	B	β		Xi	Ξ	ξ
Gamma	Γ	γ		Omicron	Ο	ο
Delta	Δ	δ		Pi	Π	π
Epsilon	Ε	ε	ε	Rho	Ρ	ρ ϑ
Zeta	Ζ	ζ		Sigma	Σ	σ ς
Eta	Η	η		Tau	Τ	τ
Theta	Θ	θ	θ	Upsilon	Υ	υ
Iota	Ι	ι		Phi	Φ	φ φ
Kappa	Κ	κ	κ	Chi	Χ	χ
Lambda	Λ	λ		Psi	Ψ	ψ
Mu	Μ	μ		Omega	Ω	ω

RUSSIAN AND ENGLISH TRIGONOMETRIC FUNCTIONS

Russian	English
sin	sin
cos	cos
tg	tan
ctg	cot
sec	sec
cosec	csc
sh	sinh
ch	cosh
th	tanh
cth	coth
sch	sech
csch	csch
arc sin	\sin^{-1}
arc cos	\cos^{-1}
arc tg	\tan^{-1}
arc ctg	\cot^{-1}
arc sec	\sec^{-1}
arc cosec	\csc^{-1}
arc sh	\sinh^{-1}
arc ch	\cosh^{-1}
arc th	\tanh^{-1}
arc cth	\coth^{-1}
arc sch	sech^{-1}
arc csch	csch^{-1}
<hr/>	
rot	curl
lg	log

GRAPHICS DISCLAIMER

All figures, graphics, tables, equations, etc. merged into this translation were extracted from the best quality copy available.

INVESTIGATION OF VELOCITY FIELD BEHIND LOW-FLYING WING WITH FUSELAGE

(Presented at Scientific and Technical Conference of Lenin Ship Building Institute (LKI), October 1969)

M. K. Bochin, Dept. of Hydromechanics; L. G. Tsvetkov, Dept. of Applied and Computer Mathematics

In this article we propose a method of investigating the velocity field behind a low-flying wing with fuselage. The value of the velocity field is necessary in calculating the aerodynamic characteristics of the tail assembly of aircraft which use the screen effect.

Numerical Calculation Method of Velocity Field

We investigate the uniform movement of a wing of finite span with a fuselage above a solid screen. The sheet of solid vortices which is formed twist, according to [1], into two vortex tip filaments, which lie upstream from the wing. The intensity and arrangement of the vortices are determined in the main velocity field behind the wing. Therefore, in our study we will ignore the stream caused by the attached wing vortex. Coordinate system $Ox'y'z'$, attached to the wing (Fig. 1), is selected such that the attached vortex of the supporting wing lies within plane $y'oz'$; the ox' axis lies downstream from the fuselage; the cy' axis vertically above it. The fuselage is assumed to have the shape of a circular finite cylinder with a zero angle of attack. Our symbols are: u_0 - velocity of undisturbed oncoming flow parallel to ox' axis and plane of screen; Γ_+ - intensity of vortex tip filaments; l - their distance from diametrical plane; e - elevation of free vortices above fuselage axis; h - distance of fuselage axis from screen; R - radius of cylindrical fuselage. Work [3] should be used as a guide in selecting the arrangement of the free vortex filaments.

In order to satisfy the condition of nonleakage on the fuselage from vortices 1 and 2 (Fig. 1) in the case of a wing and fuselage moving in an infinite fluid, according to [2] we place vortices 3 and 4 at the points of inversion inside the fuselage. In order to satisfy the boundary condition of nonpenetration in the case of a system moving near a solid screen, we map on it its mirror image relative to the plane of the screen the preceding vortex system, thus obtaining a hypothetical vortex system (vortices 5-8). In order to eliminate the violated condition of nonpenetration on the fuselage while preserving it on the screen, we use the method of successive inversion of vortices, in which each vortex of the hypothetical system (vortex A_0 , Fig. 2) is mapped in relation to the surface of the fuselage, placing at the point of inversion vortex B_1 , which is mapped relative to the screen - vortex A_1 . Then, we perform a second approximation - vortex A_1 is mapped on B_2 and B_2 - on A_2 , etc. As a result of this chains of vortices are formed inside the main and hypothetical fuselages, and in the presence of vortex A_0^* , which is symmetrical relative to the diametric plane of vortex A_0 , the same chains are formed, although this time symmetrical in relation to Π with circulation of the opposite sign. After the γ -order of approximation the "residual leakage" of the fuselage is the result of vortices A_γ and A_γ^* , which, as the approximation order increases, move closer together, reducing the velocities induced by them and thus assuring necessary accuracy in satisfying the boundary condition on the fuselage. The complete

vortex system corresponding to the studied problem is shown in Fig. 1, where dashed lines represent the chains of vortices.

Let us determine vertical downwash $w = \frac{\partial \xi}{\partial u_0}$ at point $M(x', y', z')$, after introducing the dimensionless quantity

$$\Gamma = \frac{\Gamma_+}{u_0 \ell}; \quad \bar{R} = \frac{R}{\ell}; \quad \bar{e} = \frac{e}{\ell}; \quad \bar{h} = \frac{h}{\ell}; \quad x = \frac{x'}{\ell}; \quad \xi = \frac{\xi'}{\ell} \text{ etc.} \quad (1)$$

After applying the Biot-Savart formula to the elements of the vortex system of Fig. 1, we get:

$$w = \frac{\Gamma}{4\pi} \left[\sum_{n=1}^8 (-1)^{n+1} \cdot \frac{z - \zeta_n}{r_n^2} \left(1 + \frac{x}{\sqrt{x^2 + r_n^2}} \right) + \sum_{\lambda=1}^4 \sum_{\lambda=1}^4 (-1)^{\lambda} \cdot \frac{z - \zeta_{\lambda}^I}{(r_{\lambda}^I)^2} \left(1 + \frac{x}{\sqrt{x^2 + (r_{\lambda}^I)^2}} \right) \right], \quad (2)$$

where

$$r_n = \sqrt{(x - \zeta_n)^2 + (y - \zeta_n)^2}; \quad r_{\lambda}^I = \sqrt{(x - \zeta_{\lambda}^I)^2 + (y - \zeta_{\lambda}^I)^2}; \quad (3)$$

ζ_n and ζ_n^I are the coordinates of vortices 1-8, where n is the number of the vortex according to Fig. 1.

The values of the coordinates have the form of

$$\left. \begin{aligned} \zeta_1 = \zeta_6 = -\zeta_2 = -\zeta_5 = 1; \quad \zeta_4 = \zeta_7 = -\zeta_3 = -\zeta_8 = \frac{\bar{R}^2}{1 + \bar{e}^2}; \quad \zeta_1 = \zeta_7 = \bar{e} \\ \zeta_3 = \zeta_4 = \bar{e} \frac{\bar{R}^2}{1 + \bar{e}^2}; \quad \zeta_5 = \zeta_6 = -(2\bar{h} + \bar{e}); \quad \zeta_7 = \zeta_8 = -(2\bar{h} + \bar{e} \frac{\bar{R}^2}{1 + \bar{e}^2}) \end{aligned} \right\}, \quad (4)$$

η_λ^r and ζ_λ^r are the coordinates of the vortices in the chain, where λ is the number of the chain (according to Fig. 1); r - the number of the vortex in the chain (or order of approximation).

The coordinates of the vortices in the chains in shifting from approximation r to approximation $r + 1$ when $\lambda = 6$ and $\lambda = 7$ are calculated according to the formulas:

$$\zeta_\lambda^{r+1} = \frac{\bar{R}^2 \cdot \zeta_\lambda^r}{(\zeta_\lambda^r)^2 + (2\bar{h} + \eta_\lambda^r)^2}; \quad \eta_\lambda^{r+1} = -\frac{\bar{R}^2(2\bar{h} + \eta_\lambda^r)}{(\zeta_\lambda^r)^2 + (2\bar{h} + \eta_\lambda^r)^2}. \quad (5)$$

Then, the coordinates of the vortices in the chains for the given order of approximation ($r = \text{const}$) are related to ζ_6^r ; ζ_7^r ; η_6^r and η_7^r by relationships:

$$\left. \begin{aligned} \eta_1^r = \eta_2^r = -(2\bar{h} + \eta_6^r); \quad \eta_5^r = \eta_6^r; \quad \zeta_2^r = \zeta_5^r = -\zeta_1^r = -\zeta_6^r; \\ \eta_4^r = \eta_3^r = -(2\bar{h} + \eta_7^r); \quad \eta_8^r = \eta_7^r; \quad \zeta_3^r = \zeta_8^r = -\zeta_4^r = -\zeta_7^r \end{aligned} \right\}. \quad (6)$$

The coordinates of the first vortices in the chains ($r = 1$) when $\lambda = 6$ and $\lambda = 7$ are determined by formulas (5) through coordinates with corresponding indices $n = 6$ and $n = 7$, which are calculated according to formula (4).

By using the Bernoulli equation and applying the Biot-Savart formula to the elements of the vortex system of Fig. 1, we get a formula for calculating the distribution of the pressure coefficient over the surface of a cylindrical fuselage:

$$\bar{p} = -\frac{\Gamma^2}{16\pi^2} \left[\sum_{n=1}^N (-1)^{n+1} \frac{\bar{R} - \zeta_n \cos \theta - \zeta_n^* \sin \theta}{\rho_n^2} \left(1 + \frac{x}{\sqrt{x^2 - \rho_n^2}} \right) + \sum_{k=1}^K \sum_{\lambda=1}^N (-1)^{\lambda} \frac{\bar{R} - \zeta_\lambda^* \cos \theta - \zeta_\lambda^* \sin \theta}{(\rho_\lambda^*)^2} \left(1 + \frac{x}{\sqrt{x^2 + (\rho_\lambda^*)^2}} \right) \right]^2 \quad (7)$$

where

$$\rho_n = \sqrt{(\bar{R} \cos \theta - \zeta_n)^2 + (\bar{R} \sin \theta - \zeta_n^*)^2}; \quad \rho_\lambda^* = \sqrt{(\bar{R} \cos \theta - \zeta_\lambda^*)^2 + (\bar{R} \sin \theta - \zeta_\lambda)^2}; \quad (8)$$

θ - is the polar angle of the studied point on the fuselage surface, reckoned from the horizontal plane.

In calculating quantities ω and \bar{p} according to formulas (2) and (7) we should limit ourselves to approximation $\gamma = k$, where the increment in the sum with respect to γ becomes lower than the required accuracy of calculating quantities ω or \bar{p} .

According to this method a calculation was performed for a section of infinite distance downstream for the distribution of the reduced coefficient of pressure $\frac{\bar{p}}{\rho U^2}$ over the surface of the fuselage

(Fig. 3) and the reduced vertical downwash $\frac{w}{V}$ along the wing span (Fig. 4) for the following calculated parameters:

$$\bar{R} = \frac{R}{\ell} = 0,20; \quad \bar{h} = \frac{h}{\ell} = 0,25; \quad \bar{e} = 0.$$

Investigation of Velocity Field on EGDA Device

For a section of infinite distance along the stream the investigation of the velocity field behind a low-flying wing with a cylindrical fuselage can be done on a plane electrohydrodynamic analogy device [the EGDA], as shown in Fig. 5.

The symbols in Fig. 5: 1 - sheet of electroconductive paper, 2 - bus, 3 - electrode which simulates vortex, 4 - sheet of electroconductive paper which simulates plane undisturbed flow, 5 - direct current source, 6 - galvanometer, 7 - probe.

Simulation of the free vortex flowing off of the wing tip is done by an electrode (source of electrical field). Observance of the boundary conditions requires that the contour (of fuselage and screener) in this analogy be made from a conductor. The symmetry of the flow in relation to the diametric plane is assured by installing a bus in this plane. In this case the force lines of the electrical field will correspond to the equipotential lines in the stream of

fluid, the equipotential lines of the electrical field - to the flow lines in the fluid.

The posed problem for a section of infinite length was modeled on the EGDA. The following was obtained: the field of vertical downwashes over the span of the wing (compared with calculations on Fig. 4), field of vertical downwashes at location of tail assembly (Fig. 6), and pattern of flow lines (Fig. 7) for following parameters: $\bar{R} = 0,20$; $\bar{h} = 0,25$ and $\bar{e} = 0$.

CONCLUSIONS

1. The experiments performed on the electrohydrodynamic analogy device verified the proposed method for calculating the velocity field behind a low-flying wing with cylindrical fuselage both qualitatively and quantitatively.
2. The cylindrical fuselage substantially affects the velocity field near the fuselage, within a region of 2-2.5 times its radius, decreasing or increasing the vertical downwash depending on the location of the studied point.
3. When the system of wing and fuselage approach the screen, the rarefaction curve on the surface of the fuselage, which is caused by the vortex sheet flowing off of the wing, decreases on one hand,

while on the other there occurs a redistribution in this curve, as a result of which additional lifting force develops on the fuselage. This deduction must also qualitatively be verified by the pattern of flow lines obtained on the FGDA.

BIBLIOGRAPHY

1. ГОЛУБЕВ В.В. Теория крыла аэроплана конечного размаха. ЦАГИ, вып. 108, 1931.
2. ДЮРЭНД В.Ф. Аэродинамика. Т.4. М. Оборонгиз, 1940.
3. ТРЕШКОВ В.К. Исследование поля вертикальных скосов за низколетящим крылом. Тр.ЛКИ, вып. LXIII, 1968.

Fig. 1.

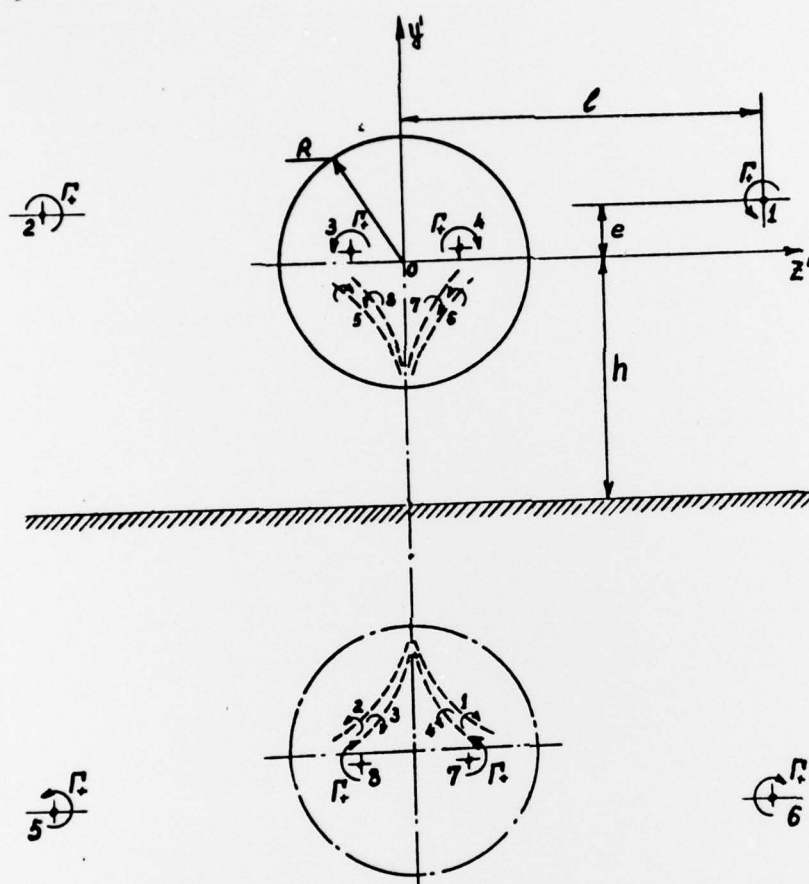
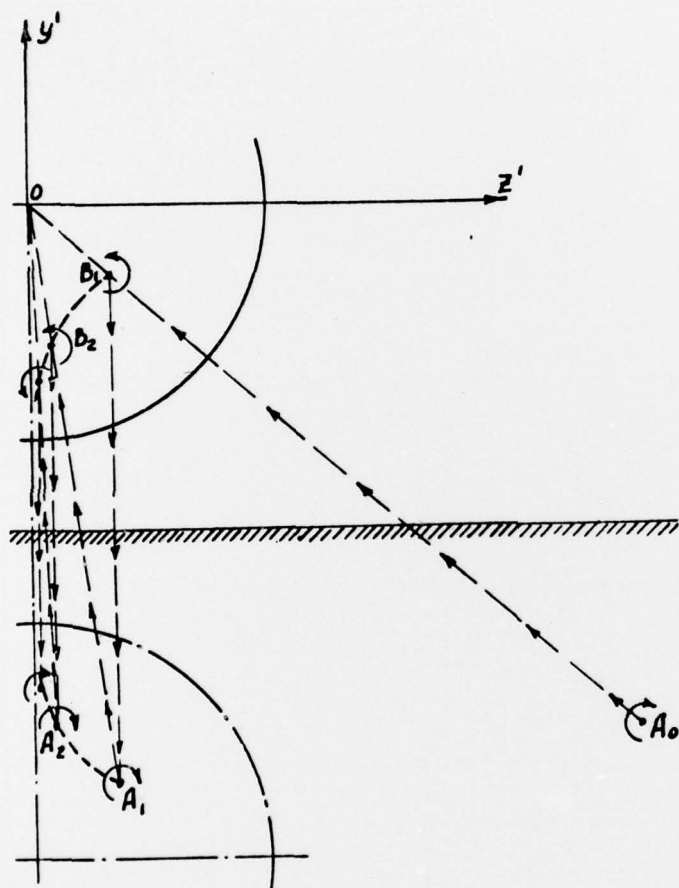


Fig. 2.



DCC = 0531

12

Fig. 3.

(1) Масштаб $\frac{\bar{p}}{g^2}$
0 4005 4010

Key: (1) Scale \bar{p}/g^2 .

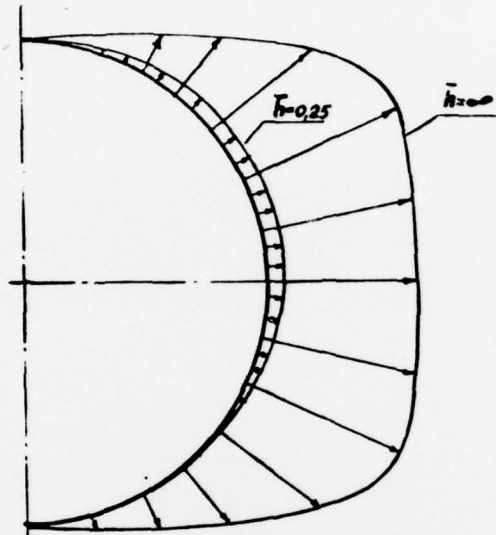
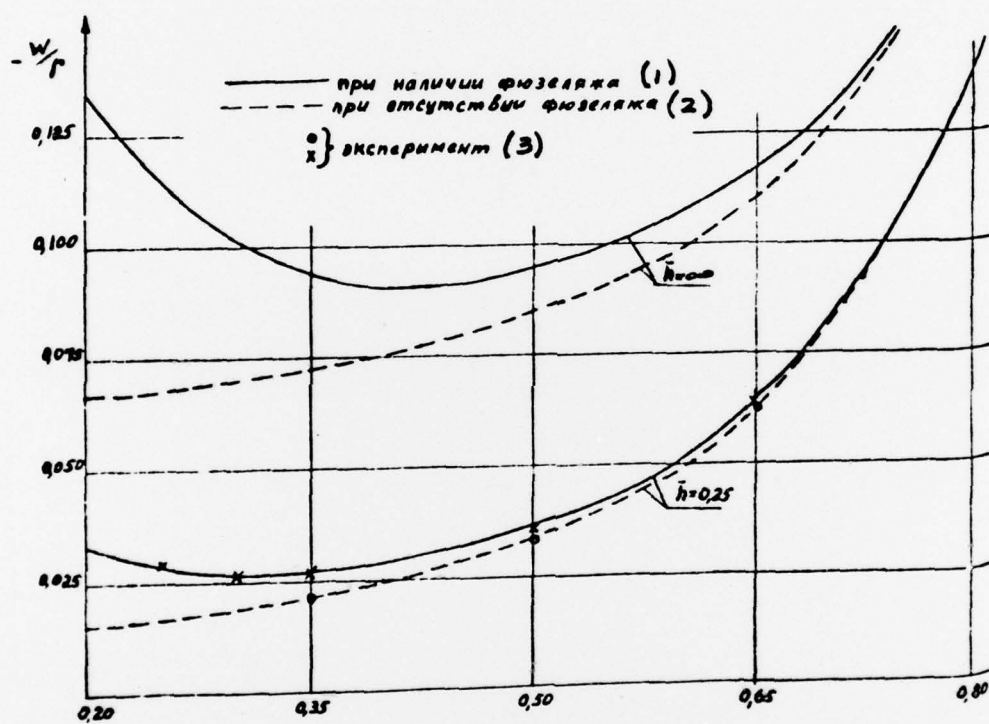


Fig. 4.

Key: (1) with fuselage, (2) without fuselage, (3) experiment.



DCC = 0531

14

Fig. 5.

Key: (1) Screen.

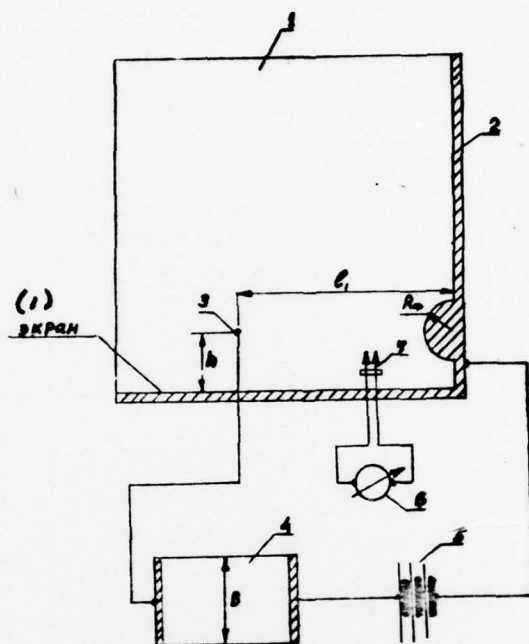


Fig. 6.

Key: (1) without fuselage, (2) with fuselage.

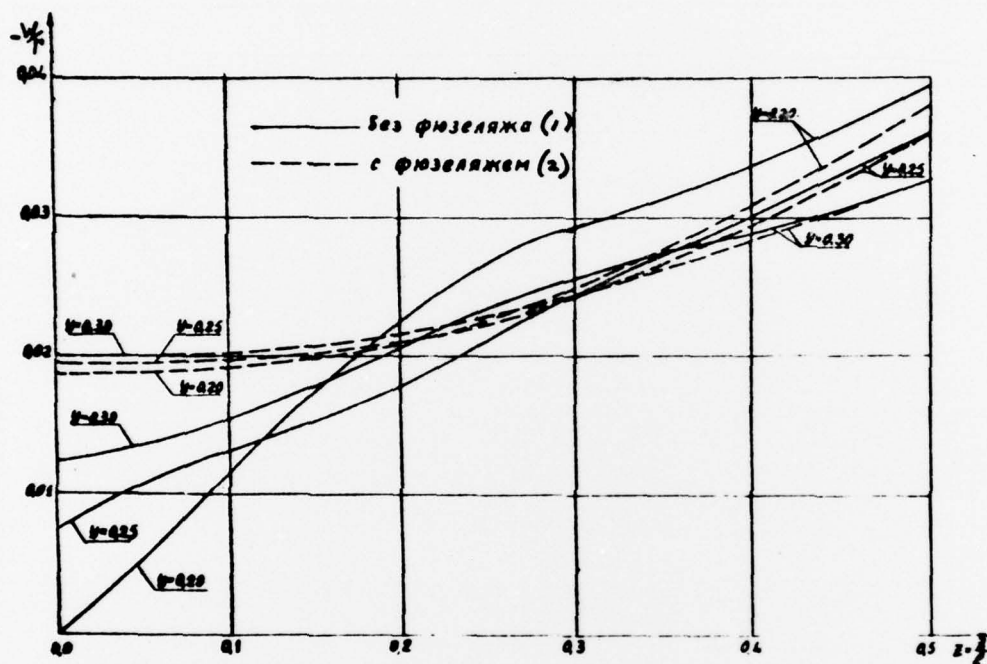
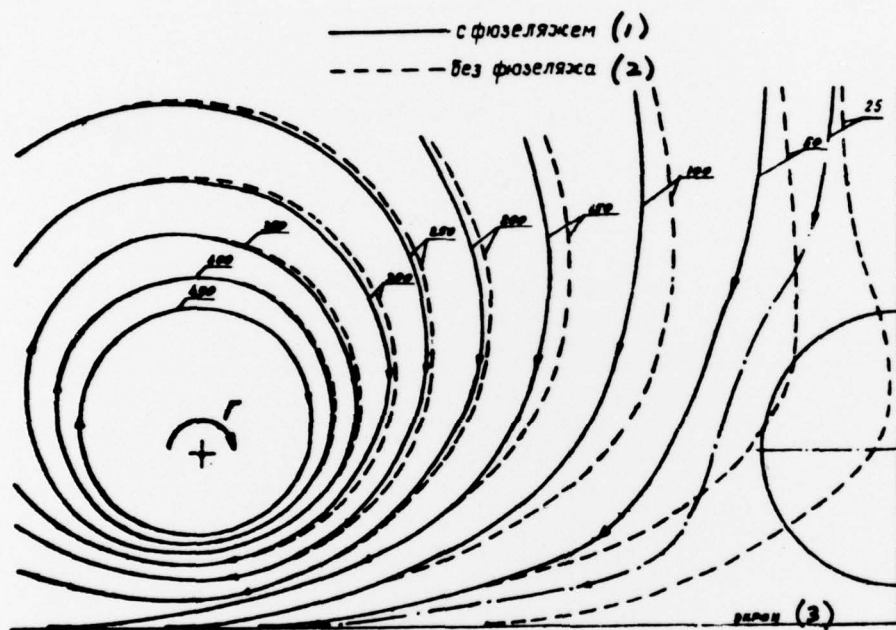


Fig. 7.

Key: (1) without fuselage, (2) with fuselage, (3) screen.



UNCLASSIFIED

SECURITY CLASSIFICATION OF THIS PAGE (When Data Entered)

REPORT DOCUMENTATION PAGE		READ INSTRUCTIONS BEFORE COMPLETING FORM
1. REPORT NUMBER FTD-ID(RS)I-0531-77	2. GOVT ACCESSION NO.	3. RECIPIENT'S CATALOG NUMBER
4. TITLE (and Subtitle) INVESTIGATION OF VELOCITY FIELD BEHIND LOW-FLYING WING WITH FUSELAGE		5. TYPE OF REPORT & PERIOD COVERED Translation
		6. PERFORMING ORG. REPORT NUMBER
7. AUTHOR(s) M. K. Bochyn, L. G. Tsvetkov		8. CONTRACT OR GRANT NUMBER(s)
9. PERFORMING ORGANIZATION NAME AND ADDRESS Foreign Technology Division Air Force Systems Command U. S. Air Force		10. PROGRAM ELEMENT, PROJECT, TASK AREA & WORK UNIT NUMBERS
11. CONTROLLING OFFICE NAME AND ADDRESS		12. REPORT DATE 1970
		13. NUMBER OF PAGES 16
14. MONITORING AGENCY NAME & ADDRESS (if different from Controlling Office)		15. SECURITY CLASS. (of this report) UNCLASSIFIED
		15a. DECLASSIFICATION/DOWNGRADING SCHEDULE
16. DISTRIBUTION STATEMENT (of this Report) Approved for public release; distribution unlimited.		
17. DISTRIBUTION STATEMENT (of the abstract entered in Block 20, if different from Report)		
18. SUPPLEMENTARY NOTES		
19. KEY WORDS (Continue on reverse side if necessary and identify by block number)		
20. ABSTRACT (Continue on reverse side if necessary and identify by block number)		
01;20		

DISTRIBUTION LIST

DISTRIBUTION DIRECT TO RECIPIENT

ORGANIZATION	MICROFICHE	ORGANIZATION	MICROFICHE
A205 DMATC	1	E053 AF/INAKA	1
A210 DMAAC	2	E017 AF/ RDXTR-W	1
B344 DIA/RDS-3C	8	E404 AEDC	1
C043 USAMIA	1	E408 AFWL	1
C509 BALLISTIC RES LABS	1	E410 ADTC	1
C510 AIR MOBILITY R&D	1	E413 ESD	2
LAB/FIO		FTD	
C513 PICATINNY ARSENAL	1	CCN	1
C535 AVIATION SYS COMD	1	ETID	3
C557 USAIIC	1	NIA/PHS	1
C591 FSTC	5	NICD	5
C619 MIA REDSTONE	1		
D008 NISC	1		
H300 USAICE (USAREUR)	1		
P005 ERDA	1		
P055 CIA/CRS/ADD/SD	1		
NAVORDSTA (50L)	1		
NAWPNSCEN (Code 121)	1		
NASA/KSI	1		
[REDACTED]	1		
AFIT/LD	1		

FTD-ID(RS)I-0531-77

Preceding Page BLANK -